DOI: 10.1002/ange.200802558

Polymerization Catalysis

Formation of Nanotubular Methylaluminoxanes and the Nature of the Active Species in Single-Site α-Olefin Polymerization Catalysis**

Mikko Linnolahti, John R. Severn, and Tapani A. Pakkanen*

Dedicated to the Catalysis Society of Japan on the occasion of its 50th anniversary

Methylaluminoxane (MAO) is a critical component in single-site α-olefin polymerization catalysis, profoundly influencing the activity, stereoselectivity, and molecular weight capability of the catalytic system.[1] The main task of MAO is to activate the catalyst precursor, thereby generating the active species, a prerequisite for initiation of the polymerization process. Unfortunately, the structure of the active component is not well understood, and the complex structural characteristics of MAO have remained elusive despite many experimental and theoretical studies.[2,3] The inability to tie down the structure of the active component has hindered the complete understanding and control of the polymerization process, as well as rational cocatalyst optimization, where most development has consequently taken place around alternative activators.[1] Herein we describe the formation and molecular structures of nanotubular MAOs. Quantum chemical calculations show that the MAO nanotubes possess higher thermodynamic stability than previously reported structural alternatives. The ends of the MAO tubes, which act as active sites, are capped with trimethylaluminum (TMA) and are able to activate catalyst precursors for initiation of olefin polymerization.

The lack of a precise structural characterization of MAO has led to many proposals about its structure. Although there is no generally accepted structure, the proposed cage structures with four-coordinate Al and three-coordinate O centers, comprised only of Al–O and Al–Me bonds, are most widely accepted.[4] The current understanding of the structural motifs of MAO is largely based on the experimental evidence on other alkyl aluminoxanes with bulkier alkyl groups,[5] and on theoretical studies on its structural alternatives.[3,6] With the rapid increase in computational power, quantum chemical calculations have become an increasingly powerful tool for the structural characterization of MAO.

Nonetheless, the structural characterization of MAO is very challenging also from a computational point of view. MAO is prepared by hydrolysis of TMA,[1] and the polymerization reactions lead to a variety of structures. The situation is further complicated by the dimer structure of TMA,[7] in which the bridging pentavalent methyl groups introduce electron deficient three-centered two-electron bonds. The dimer structure of TMA has turned out to be one of the Achilles' heels of density functional theory, which has been widely employed in theoretical studies of MAO.[3] The failure of density functional theory to reproduce the experimental finding of the dimerization of TMA[8] is unfortunate because of the presence of associated TMA in MAO. This problem was the starting point of the present approach: the choice of an appropriate computational method. Electronic energies and enthalpies, as well as Gibbs free energies for dimerization of TMA are given in Table 1 at various levels of theory together with comparisons with experimental results. The very common B3LYP method is here chosen to represent density functional theory. MP2 produces dimerization energies in close agreement with both the CCSD(T) method and the experimental results, whereas B3LYP deviates significantly. As a consequence, the MP2/def-TZVP method was employed in the further studies reported below.

Table 1: Dimerization of TMA: Electronic energies (ΔE) and enthalpies (ΔH), as well as Gibbs free energies (ΔG) [kJ mol^{-1}].[a]

Method	ΔE	ΔH	ΔG
B3LYP/6-311G**	−35.2	−27.5	50.1
MP2/def-TZVP	−89.3	−80.2	−14.0
CCSD(T)/def2-QZVPP[b]	−93.2	−84.1	−17.9
Experimental[7]		−85.4	−31.2

[a] $T = 298.15$ K, $p = 0.1$ MPa; for a more comprehensive version of Table 1, see the Supporting Information. [b] Single-point energies on the MP2/def-TZVP-optimized structures; thermal corrections taken from the MP2/def-TZVP calculations.

The considered reaction pathways for the formation of MAOs from the hydrolysis of TMA are illustrated in Figure 1, and the energy parameters are reported in Table 2. The reaction pathways are highly exothermic all the way through to the MAO products. Hydrolysis of the TMA dimer produces a complex of TMA and H_2O, which undergoes intramolecular elimination of methane to yield $AlMe_2OH$. The $AlMe_2OH$ acts as a monomer for polymerization of MAO and can react further either with other $AlMe_2OH$ monomers or with TMA. A reaction between two $AlMe_2OH$ molecules produces a dimer with a four-membered Al_2O_2 ring. Moving on from the dimer, subsequent reactions with the monomers produce cage-like structures, and reactions with TMA terminate the

[*] Dr. M. Linnolahti, Prof. T. A. Pakkanen
Department of Chemistry, University of Joensuu
P.O. Box 111, 80101 Joensuu (Finland)
Fax: (+358) 13-251-3390
E-mail: mikko.linnolahti@joensuu.fi
Dr. J. R. Severn
Borealis Polymers Oy, P.O. Box 330, 06101 Porvoo (Finland)

[**] Dr. Antti Karttunen (University of Joensuu) is thanked for technical assistance with the calculations.

Supporting information for this article is available on the WWW under http://dx.doi.org/10.1002/anie.200802558.

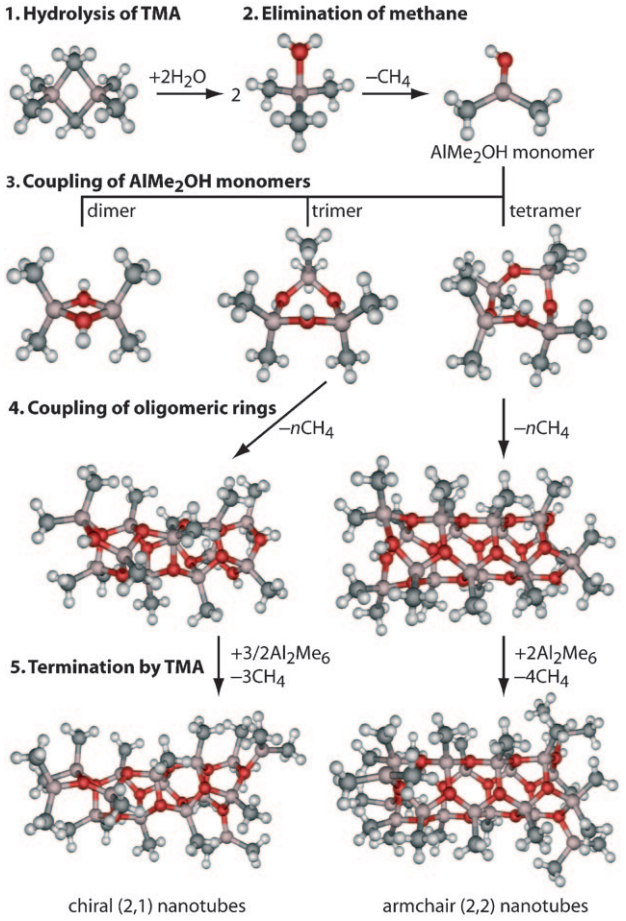

Figure 1. Reaction pathways for the formation of nanotubular MAOs.

growth to yield the final MAO products. This particular reaction pathway has been studied in detail by Hall and co-workers.[9]

Aluminoxanes prefer six-membered Al_3O_3 rings over four-membered Al_2O_2 rings.[3] The strained Al_2O_2 rings are present both in the dimer and in the subsequently formed cage structures of MAO. Because of the strain, coupling of three monomers to produce a $(AlMe_2OH)_3$ trimer composed of a six-membered ring is thermodynamically favored over dimerization (Table 2). In the favored conformation of the trimer, two of the three OH groups point in the same direction. Likewise, four monomers can couple to form a tetrameric ring. The orientations of the adjacent OH groups in the favored conformation alternate up and down. The formation of the tetramer ring is equally favorable to the formation of the trimer, whereas the formation of a pentameric ring is already less favorable.

Moving on from the trimer and tetramer, subsequent monomer insertions, described herein as trimer–trimer and tetramer–tetramer couplings, lead to the formation of nanotubular structures. Adopting the naming conventions of carbon nanotubes,[10] these configurations are termed chiral (2,1) for the trimer and armchair (2,2) for the tetramer. As the couplings of the oligomeric rings are accompanied by elimination of methane they are highly exothermic. Coupling of the tetramers is somewhat more favorable because of the difference in the curvatures of the (2,1) and (2,2) nanotubes; the latter is more optimal for sp^3 hybridization. How long the tubes grow is determined by competition between $AlMe_2OH$ and TMA; reactions with TMA terminate the tube growth to yield the final MAO product. Reaction with TMA is somewhat favored over reaction with $AlMe_2OH$, and is also more exothermic for (2,2) than for (2,1) nanotubes.

How long can the tubes actually grow and what are the thermodynamic stabilities of the MAO products? To provide answers to the questions, it is useful to write the molecular formula of the MAOs in the form $(AlOMe)_n(AlMe_3)_m$ to describe the amount of associated TMA. We know from experimental work that TMA dimerizes,[7] and because we are using a computational method (MP2) capable of reproducing the dimerization correctly, we can extract the energy of the TMA dimer from the MAOs. This calculation leaves us with energy per AlOMe unit, which is what can be compared with other proposed structures. In this case we compare it with the most stable structure, the $(AlOMe)_{12}$ cage, suggested by Ziegler and co-workers as the most stable MAO at all temperatures.[6b,c]

Electronic energies and Gibbs free energies of the (2,1) and (2,2) nanotubes are illustrated in Figure 2. The stabilities of the nanotubes are given with respect to the $(AlOMe)_{12}$ cage, and are plotted as a function of the number of AlOMe units. In terms of electronic energies, both (2,1) and (2,2) nanotubes are favored over the $(AlOMe)_{12}$ cage, except for the shortest (2,1) tube. The (2,2) tubes are clearly preferred, because of the nearly optimal sp^3 hybridization, as pointed out above. The relative stabilities of the (2,1) tubes improve as a function of the length of the tube. In contrast, the (2,2) tubes reach a minimum in energy at dodecamer ($Al_{16}O_{12}Me_{24}$). The (2,2) nanotubes longer than the dodecamer are destabilized by repulsion between the adjacent methyl groups. In this regard, the best configuration for the MAO nanotubes would be zigzag (4,0),[11] but its formation would require reorganization of the AlOMe core, which may not be kinetically feasible.

Interestingly, the molecular formula of the dodecamer ($Al_{16}O_{12}Me_{24}$) is exactly the one originally proposed by Sinn.[4] Its molecular weight of 985 $g\,mol^{-1}$ matches well with the experimental measurements of about 1000 $g\,mol^{-1}$.[4] Also the C:Al:O ratio of 1.5:1:0.75 is equal to the experimental molecular formula of -$[Me_{1.4-1.5}AlO_{0.80-0.75}]_n$-.[12] The length of $Al_{16}O_{12}Me_{24}$ (14.8 Å) agrees with the spatial size estimate by Talsi and co-workers,[13a] who suggest a diameter of 13–15 Å for MAO. Hansen et al.[13b] reported an estimate of 19–20 Å, which would better comform with the length of the hexadecamer ($Al_{20}O_{16}Me_{28}$; 17.5 Å), which has a molecular weight of 1217 $g\,mol^{-1}$ and C:Al:O ratio of 1.4:1:0.8. The estimated effective radius of $[Cp_2Zr(\mu\text{-}Me_2)AlMe_2]^+Me\text{–}MAO^-$ (Cp = cyclopentadienyl) is also of the same magnitude (12.2–14.4 Å).[13c] Moreover, there is experimental evidence of terminal -$OAlMe_2$ groups[14] and bridging methyl groups,[15] both of which are present in the caps of the nanotubes. Summing up the agreements with the high stability and the feasibility of formation from the hydrolysis of TMA, the nanotubular armchair (2,2) dodecamer ($Al_{16}O_{12}Me_{24}$), per-

Table 2: Energy parameters [kJ mol^{-1}] for reactions leading to the formation of nanotubular MAOs.[a,b]

Reaction	ΔE	ΔG	ΔG per Al[c]
1. Hydrolysis of TMA			
$Al_2Me_6 + 2\,H_2O \rightarrow 2\,AlMe_3OH_2$	−60.3 (−64.0)	−30.0 (−33.8)	−15.0 (−16.9)
2. Elimination of methane			
$AlMe_3OH_2 \rightarrow AlMe_2OH + CH_4$	−77.0 (−82.3)	−119.6 (−124.9)	−119.6 (−124.9)
3. Coupling of $AlMe_2OH$ monomers			
dimer $2\,AlMe_2OH \rightarrow Al_2Me_4O_2H_2$	−246.3 (−242.9)	−174.1 (−170.7)	−87.0 (−85.3)
trimer $3\,AlMe_2OH \rightarrow Al_3Me_6O_3H_3$	−435.6 (−432.2)	−299.8 (−296.4)	−99.9 (−98.8)
tetramer $4\,AlMe_2OH \rightarrow Al_4Me_8O_4H_4$	−601.2	−396.9	−99.2
4. Coupling of oligomeric rings			
four trimers, chiral (2,1): $12\,AlMe_2OH \rightarrow Al_{12}Me_{15}O_{12}H_3 + 9\,CH_4$	−3060.5	−2609.7	−217.5
four tetramers, armchair (2,2): $16\,AlMe_2OH \rightarrow Al_{16}Me_{20}O_{16}H_4 + 12\,CH_4$	−4229.4	−3569.6	−223.1
5. Termination by TMA			
dodecamer, chiral (2,1): $Al_{12}Me_{15}O_{12}H_3 + 3/2\,Al_2Me_6 \rightarrow Al_{15}O_{12}Me_{21} + 3\,CH_4$	−438.2	−689.6	−229.9
hexadecamer, armchair (2,2): $Al_{16}Me_{20}O_{16}H_4 + 2\,Al_2Me_6 \rightarrow Al_{20}O_{16}Me_{28} + 4\,CH_4$	−636.2	−978.1	−244.5

[a] $T = 298.15$ K, $p = 0.1$ MPa; for a more comprehensive version of Table 2, see the Supporting Information. [b] MP2/def-TZVP level of theory (CCSD(T)/def2-TZVP//MP2/def-TZVP in parentheses, thermal corrections taken from the MP2/def-TZVP calculations). [c] Gibbs free energy divided by the number of Al atoms involved in the reaction.

haps together with the hexadecamer ($Al_{20}O_{16}Me_{28}$), appear to be likely contributors to the structure of MAO.

The structure of MAO appears to be very sensitive to temperature. At room temperature, the $Al_{16}O_{12}Me_{24}$ nanotube is thermodynamically favored over the $(AlOMe)_{12}$ cage, previously considered the most stable MAO at all temperatures. However, the energy difference in favor of the nanotube is clearly smaller at 298.15 K (ΔG) than at 0 K (ΔE), suggesting dissociation of the associated TMA at elevated temperatures. We calculated the limiting temperature to be around 370 K. The size of MAO was observed experimentally to decrease upon heating,[13a,b] suggesting dissociation of TMA. The release of TMA upon thermal destruction of MAO has actually been observed experimentally.[16] In this case, the polymerization rate suddenly drops upon heating MAO to about 370 K and above, and remains practically constant below this limiting temperature. This result provides clear evidence of the role of associated TMA in the cocatalytic activity of MAO.

To test if the proposed MAO nanotubes could possess cocatalytic activity toward olefin polymerization, we considered reactions between a $[Cp_2ZrMe_2]$ zirconocene and the armchair (2,2) $Al_{16}O_{12}Me_{24}$. Two exothermic reactions were located, and their products are shown in Figure 3. Representative of the complexity of the MP2

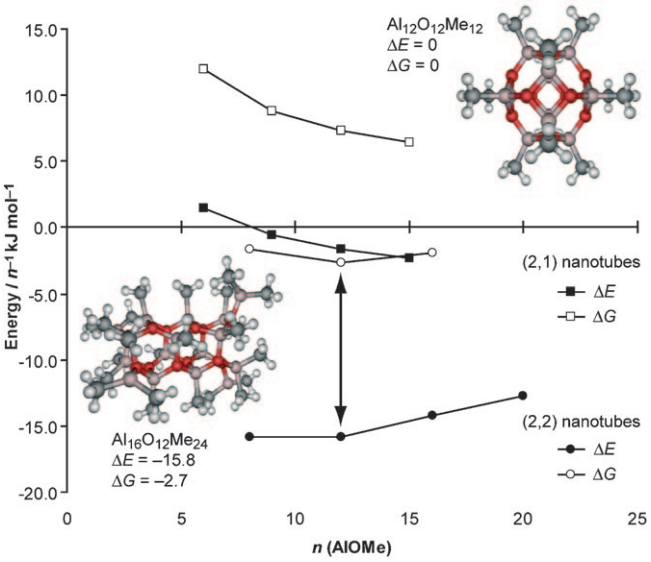

Figure 2. Stabilities of nanotubular MAOs relative to the tetrahedral $Al_{12}O_{12}Me_{12}$ cage[6b,c] ($T = 298.15$ K, $p = 0.1$ MPa).

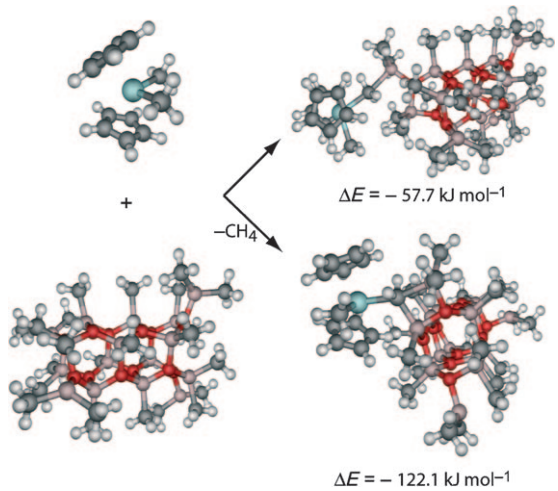

Figure 3. Activation (top) and deactivation (bottom) of a $[Cp_2ZrMe_2]$ catalyst by MAO.

calculations, the structure optimizations of the two reaction products took about a month each when run on 64 parallel processors (2.66 GHz Intel Xeon EM64T).

The reactions lead to metallocene–MAO complexes, in which the bridging pentavalent carbon atoms play a central role. Direct reaction between the methylated zirconocene precursor and MAO (Figure 3, top) breaks the Al–C bond to the bridging carbon atom. The formed three-coordinated aluminum center is capable of partially abstracting the methyl group of the zirconocene, thereby reducing its electron deficiency. The partially abstracted methyl group appears to be in a delicate balance between the Zr and Al centers; the bond lengths are 2.35 Å and 2.26 Å for Zr–C and Al–C, respectively. Under these circumstances, it seems plausible that an incoming monomer can replace the methyl group, thereby forming an olefin-coordinated zirconocene cation and a noncoordinated $MeMAO^-$ anion in its close proximity. Within the framework of the current understanding of the single-site olefin polymerization process, a system of this kind would polymerize olefins, and, hence, the ion pair illustrated in the top right of Figure 3 should be the active species.[17]

In the other exothermic reaction (Figure 3, bottom), the dimethylated zirconocene undergoes α-hydrogen transfer to MAO, eliminating the transferred hydrogen atom and the bridging methyl group in the form of methane and leaving the zirconocene cation tightly bound to the MAO through a bridging methylene group (CH_2). The Zr–C and Al–C bond lengths (2.35 Å and 2.19 Å, respectively) are not much different from those in the above reaction, but the coordination is stronger, as suggested by the reaction energy of $-122\ kJ\,mol^{-1}$, compared to $-57.7\ kJ\,mol^{-1}$ above. The coordination may actually be too strong for the $Zr–CH_2$ bond to be replaced by the monomer. In light of the strength of the coordination and the experimental evidence for the formation of bridging methylene groups through methane elimination,[18] which has been attributed as the cause of catalyst deactivation,[19] the species in bottom right of Figure 3 is likely to be a product of deactivation. Further calculations will be required, however, to verify if this is the case. In this context, it is also worth pointing out that two distinct but different zirconocene–MAO ion pairs have been recently observed by Brintzinger and co-workers.[20] The ion pairs bind with different strengths, and there is about an order of magnitude difference in the equilibrium constants for displacement of the MAO anion from the cationic Zr center. The observations may be relevant to the present calculations.

Turning back to the active species (Figure 3 top right), an important question is how to alter the dedicate balance of the abstracted methyl group between the Zr and Al centers. The use of a solvent, such as toluene, is one feasible way to separate the cation and anion. Another way is to modify the ligand structure of the catalyst. Strongly electron-donating ligands have been shown to stabilize the cationic metal center, facilitating cation–anion separation and thereby leading to enhanced polymerization activities due to a lower energy activation step.[21] Yet another way is to modify the structure of the cocatalyst. The bridging methyl groups play a critical role in this respect. Unlike in the structure of TMA, in which the bridging methyl groups are equally shared by both aluminum centers, the methyl groups are located closer to one aluminum center in the case of MAO. This situation has the consequence that TMA does not act as an activator whereas MAO does, as the other aluminum center of the methyl bridge is left electron-deficient and is thus capable of abstracting the methyl group from the catalyst. The key questions concerning future cocatalyst development are how to increase the electron deficiency and Lewis acidity of the active aluminum center further and how to prepare such molecules.

In summary, we have described the formation and molecular structures of nanotubular MAOs, which are thermodynamically favored over the previously proposed structure of MAO. The nanotubular MAOs readily form in polymerization reactions between water and TMA, leading to a wide variety of species, of which an armchair (2,2) dodecamer ($Al_{16}O_{12}Me_{24}$) appears to be of particular relevance. The molecular weight and chemical composition of the described $Al_{16}O_{12}Me_{24}$ molecule are in a striking agreement with experimental measurements. Most importantly, nanotubular $Al_{16}O_{12}Me_{24}$ is capable of activating a single-site metallocene catalyst for polymerization of α-olefins.

Received: June 2, 2008
Published online: August 29, 2008

Keywords: ab initio calculations · aluminum · nanostructures · polymerization · structure elucidation

[1] a) E. Y.-X. Chen, T. J. Marks, *Chem. Rev.* **2000**, *100*, 1391 – 1394; b) J.-N. Pédeutour, K. Radhakrishnan, H. Cramail, A. Deffieux, *Macromol. Rapid Commun.* **2001**, *22*, 1095 – 1123; c) M. Bochmann, *J. Organomet. Chem.* **2004**, *689*, 3982 – 3998.
[2] S. Pasynkiewicz, *Polyhedron* **1990**, *9*, 429 – 453.
[3] E. Zurek, T. Ziegler, *Prog. Polym. Sci.* **2004**, *29*, 107 – 148.
[4] H. Sinn, *Macromol. Symp.* **1995**, *97*, 27 – 52.
[5] a) M. R. Mason, J. M. Smith, S. G. Bott, A. R. Barron, *J. Am. Chem. Soc.* **1993**, *115*, 4971 – 4984; b) C. J. Harlan, M. R. Mason, A. R. Barron, *Organometallics* **1994**, *13*, 2957 – 2969.
[6] See, for example, a) M. Ystenes, J. L. Eilertsen, J. Liu, M. Ott, E. Rytter, J. A. Støvneng, *J. Polym. Sci. Part A* **2000**, *38*, 3106 – 3127; b) E. Zurek, T. K. Woo, T. K. Firman, T. Ziegler, *Inorg. Chem.* **2001**, *40*, 361 – 370; c) E. Zurek, T. Ziegler, *Inorg. Chem.* **2001**, *40*, 3279 – 3292; d) E. Rytter, J. A. Støvneng, J. L. Eilertsen, M. Ystenes, *Organometallics* **2001**, *20*, 4466 – 4468; e) I. I. Zakharov, V. A. Zakharov, *Macromol. Theory Simul.* **2001**, *10*, 108 – 116; f) M. Linnolahti, T. N. P. Luhtanen, T. A. Pakkanen, *Chem. Eur. J.* **2004**, *10*, 5977 – 5987.
[7] M. B. Smith, *J. Organomet. Chem.* **1972**, *46*, 31 – 49.
[8] B. G. Willis, K. F. Jensen, *J. Phys. Chem. A* **1998**, *102*, 2613 – 2623.
[9] L. Negureanu, R. W. Hall, L. G. Butler, L. A. Simeral, *J. Am. Chem. Soc.* **2006**, *128*, 16816 – 16826.
[10] a) N. Hamada, S. Sawada, A. Oshiyama, *Phys. Rev. Lett.* **1992**, *68*, 1579 – 1581; b) R. Saito, M. Fujita, G. Dresselhaus, M. S. Dresselhaus, *Appl. Phys. Lett.* **1992**, *60*, 2204 – 2206.
[11] M. Linnolahti, J. R. Severn, T. A. Pakkanen, *Angew. Chem.* **2006**, *118*, 3409 – 3412; *Angew. Chem. Int. Ed.* **2006**, *45*, 3331 – 3334.
[12] D. W. Imhoff, L. S. Simeral, S. A. Sangokoya, J. H. Peel, *Organometallics* **1998**, *17*, 1941 – 1945.
[13] a) D. E. Babushkin, N. V. Semikolenova, V. N. Panchenko, A. P. Sobolev, V. A. Zakharov, E. P. Talsi, *Macromol. Chem. Phys.*

1997, *198*, 3845 – 3854; b) E. W. Hansen, R. Blom, P. O. Kvernberg, *Macromol. Chem. Phys.* **2001**, *202*, 2880 – 2889; c) D. E. Babushkin, H.-H. Brintzinger, *J. Am. Chem. Soc.* **2002**, *124*, 12869 – 12873.
[14] I. Tritto, M. C. Sacchi, P. Locatelli, S. X. Li, *Macromol. Chem. Phys.* **1996**, *197*, 1537 – 1544.
[15] J. L. Eilertsen, E. Rytter, M. Ystenes, *Vib. Spectrosc.* **2000**, *24*, 257 – 264.
[16] V. N. Panchenko, V. A. Zakharov, I. G. Danilova, E. A. Paukshtis, I. I. Zakharov, V. G. Goncharov, A. P. Suknev, *J. Mol. Catal. A* **2001**, *174*, 107 – 117.
[17] D. E. Babushkin, N. V. Semikolenova, V. A. Zakharov, E. P. Talsi, *Macromol. Chem. Phys.* **2000**, *201*, 558 – 567.
[18] S. L. Scott, T. L. Church, D. H. Nguyen, E. A. Mader, J. Moran, *Top. Catal.* **2005**, *34*, 109 – 120.
[19] W. Kaminsky, C. Strübel, *J. Mol. Catal. A* **1998**, *128*, 191 – 200.
[20] a) D. E. Babushkin, C. Naundorf, H.-H. Brintzinger, *Dalton Trans.* **2006**, 4539 – 4544; b) U. Wieser, F. Schaper, H.-H. Brintzinger, *Macromol. Symp.* **2006**, *236*, 63 – 68.
[21] M. Linnolahti, T. A. Pakkanen, *Macromolecules* **2000**, *33*, 9205 – 9214.

